Copper(II) and Nickel(II) Complexes of Dianionic and Tetraanionic Dinucleating Macrocycles

Kausik K. Nanda,[†] Anthony W. Addison,*[,†] Neil Paterson,[‡] Ekkehard Sinn,[‡,§] Laurence K. Thompson,[||] and Ushio Sakaguchi[⊥]

Departments of Chemistry, Drexel University, Philadelphia, Pennsylvania 19104-2875, The University, Hull, England HU6 7RX, U.K., Memorial University, St. John's, NF, Canada A1B 3X7, and Kumamoto Gakuen University, Kumamoto 862, Japan

Received October 1, 1997

With nickel(II) or copper(II) acetate, 2,6-bis(acetoximato)-4-methylphenol (H_2Damox) and 2,6-bis(acetoximato)-4-*tert*-butylphenol (H_2Dabox) afford molecular dinuclear complexes $[Cu_2(Damox)_2]$ (**1**), $[Ni_2(Damox)_2(MeOH)_2]\cdot$MeOH (**2**), $[Cu_2(Dabox)_2]$ (**5**) and $[Ni_2(Dabox)_2(H_2O)_2]$ (**6**). Salts of the macrocyclic tetraimine copper chelates from diacetylcresol with 1,3-diaminopropane and 1,4-diaminobutane, $[Cu_2(Dampn)]^{2+}$ and $[Cu_2(Dambn)]^{2+}$, were also examined. Pyridine solutions of **2** yielded pink crystals of $[Ni_2(Damox)_2(Py)_4]\cdot(Py)_2$ (**3a**), which effloresce pyridine to form $[Ni_2(Damox)_2(Py)_2]\cdot$Py (**3**). The pseudomacrocyclic complexes **1**, **5**, and **6** react with $BF_3\cdot Et_2O$ to form BF_2-bridged macrocyclic complexes $[Cu_2(Damfb)]$ (**4**), $[Cu_2(Dabfb)]\cdot H_2O$ (**7**), and $[Ni_2(Dabfb)]$ (**8**). Crystals of $[Ni_2(Damox)_2(Py)_4]\cdot(Py)_2$ (**3a**) are monoclinic (space group $P2_1/n$), with $a = 13.297(5)$ Å, $b = 11.240(5)$ Å, $c = 17.396(6)$ Å, $\beta = 109.03°$, $V = 2458(3)$ Å^3, $Z = 2$, $R = 0.050$, and $R_w = 0.052$. The $[Ni_2(Dabfb]$ (**8**) crystals are orthorhombic (space group *Pnma*), with $a = 11.558(6)$ Å, $b = 17.200(5)$ Å, $c = 16.058(2)$ Å, $V = 3192(3)$ Å^3, $Z = 4$, $R = 0.057$, and $R_w = 0.057$. The saddle-shaped molecules of **8** contain low-spin Ni(II). The copper(II) centers in **1**, **5**, **6**, etc., are strongly antiferromagnetically coupled with $-2J$ values in the range 550−800 cm^{-1}. The nickel(II) centers in **2** and **3** are weakly ($-2J = 3.2$ cm^{-1}) or moderately ($-2J = 19.5$ cm^{-1}) antiferromagnetically coupled, whereas **6** shows a moderate ferromagnetic interaction with $-2J = -5.1$ cm^{-1}. All the complexes are electrochemically reducible in two 1-electron steps. In CH_3CN, the mixed-valence complexes $[Cu_2(Dampn)]^+$ and $[Cu_2(Dambn)]^+$ are valence-localized. The nature of the carbon monoxide interactions with the M(I) centers is clearest for $[Cu_2(Dambn)]^{+/0}$, which in dimethylformamide solution binds two molecules of CO in a cooperative fashion.

Introduction

Since the initial reports of dinuclear copper(II) complexes with ligands derived from the condensation of 2,6-diformyl-4-methylphenol[1] or 2,6-diacetyl-4-methylphenol[2] and *N*,*N*′-diaminoalkanes or hydroxylamine, there have been extensive studies on phenoxo-bridged dinuclear macrocyclic complexes.[3−13] The focus of attention has been on probing of their redox potentials, magneto−structural relations and selective activation of substrates. A common feature of all these macrocycles is that they are dianionic and hence form dicationic dinuclear complexes of metal ions in the +2 oxidation state. Nag et al. have recently investigated the chemistry of trivalent metal ions with phenoxo-bridged tetraaza macrocycles which resulted in tricationic mixed-valence (+2, +3)[14,15] and heterodinuclear ($M^{II}-M^{III}$)[16] complexes. Tetraanionic macrocycles with similar donors should yield uncharged molecular dinuclear complexes with dipositive metal ions and offer the eventual possibility of stabilizing complexes with tripositive metals. Here we report on the properties of some macrocyclic dinuclear molecular complexes of copper(II) and nickel(II), including tetraanionic pseudomacrocyclic and macrocyclic ligands (see Chart 1).

Experimental Section

Reagents from commercial sources were used as received. 2,6-Diacetyl-4-methylphenol was synthesized according to a published

* To whom correspondence should be addressed. E-mail: addisona@dunx1.ocs.drexel.edu.
[†] Drexel University.
[‡] The University of Hull.
[§] E-mail: E.Sinn@chem.hull.ac.uk; http://www.hull.ac.uk/chemistry/homepage.html.
[||] Memorial University. E-mail: lthomp@morgan.ucs.mun.ca.
[⊥] Kumamoto Gakuen University. E-mail: sakaguchi@kumagaku.ac.jp.

(1) Pilkington, N. H.; Robson, R. *Aust. J. Chem.* **1970**, *23*, 2225.
(2) Addison, A. W. *Inorg. Nucl. Chem.* **1976**, *12*, 899.
(3) Nanda, K. K.; Das, R.; Venkatsubramanian, K.; Nag, K. *Proc. Indian Acad. Sci. (Chem. Sci.)* **1994**, *106*, 673.
(4) Atkins, A. J.; Black, D.; Blake, A. J.; Martin-Becerra, A.; Parsons, S.; Ramirez, L.; Schroeder, M. *Chem. Commun.* **1996**, 457.
(5) Nag, K. *Proc. Indian Acad. Sci. (Chem. Sci.)* **1990**, *102*, 269.
(6) Vigato, P. A.; Tamburini, S.; Fenton, D. E. *Coord. Chem. Rev.* **1990**, *106*, 25.
(7) Casellato, U.; Vigato, P. A.; Fenton, D. E.; Vidali, M. *Chem. Soc. Rev.* **1978**, *8*, 199.
(8) Groh, S. E. *Isr. J. Chem.* **1976**/**77**, *15*, 277.
(9) Bell, M.; Edwards, A. J.; Hoskins, B. F.; Kachab, E. H.; Robson, R. *J. Am. Chem. Soc.* **1989**, *111*, 3603.
(10) Tandon, S. S.; Thompson, L. K.; Bridson, J. N. *J. Chem. Soc., Chem. Commun.* **1992**, 911.
(11) Sakayama, H.; Matoda, K.; Okawa, H.; Kida, S. *Chem. Lett.* **1991**, 1133.
(12) Tandon, S. S.; McKee, V. *J. Chem. Soc., Chem. Commun.* **1988**, 385.
(13) Yonemura, M.; Matsumura, Y.; Furutachi, H.; Ohba, M.; Okawa, H. *Inorg. Chem.* **1997**, *36*, 2711.
(14) Das, R.; Nanda, K. K.; Paul, I.; Baitalik, S.; Nag, K. *Polyhedron* **1994**, *13*, 2639.
(15) Dutta, S. K.; Ensling, J.; Werner, R.; Floerke, U.; Haase, W.; Gütlich, P.; Nag, K. *Angew. Chem., Int. Ed. Engl.* **1997**, *36*, 152.
(16) Dutta, S. K.; Werner, R.; Floerke, U.; Mohanta, S.; Nanda, K. K.; Haase, W.; Nag, K. *Inorg. Chem.* **1996**, *35*, 2292.

S0020-1669(97)01243-3 CCC: $15.00
Published on Web 02/20/1998

Chart 1

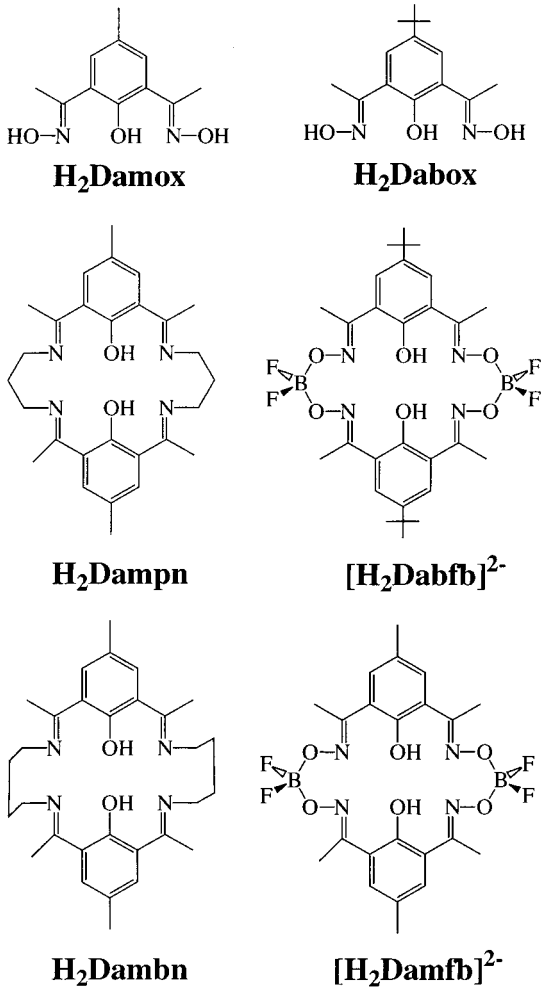

procedure.[17] Acetonitrile, dichloromethane, and *N*,*N*-dimethylformamide (DMF) were purified by distillation off P_4O_{10}, K_2CO_3, or CaH_2, respectively, under an N_2 atmosphere or in vacuo (DMF). Elemental microanalyses were performed by Robertson Microanalytical Laboratories (Madison, NJ) and Galbraith Laboratories Inc. (Knoxville, TN).

2,6-Diacetyl-4-*tert*-butylphenol. CH_3COCl (55 mL, 0.72 mol) was added dropwise over a period of 3 h to a chilled, stirred mixture of $AlCl_3$ (192 g, 1.44 mol), 4-*tert*-butylphenol (36 g, 0.24 mol), and dry nitrobenzene (250 mL) in a 2 L flask in an ice−water bath. The temperature was then raised to 65- 70 °C, and the reaction was allowed to continue overnight, following which the reaction mixture was cooled with ice and ice-cold aqueous HCl (6 M, 500 mL) was added slowly with vigorous stirring. The contents of the flask were allowed to separate overnight, and most of the nitrobenzene in the organic phase was then steam-distilled off. The phenolics were extracted with aqueous KOH, and the extract was acidified with 6 M HCl and back-extracted with ether (3 × 100 mL). After the ether extract was dried over Na_2SO_4 and the ether was rotary evaporated off, the brown viscous liquid residue was vacuum-distilled. The yellow liquid product crystallized after refrigeration and was recrystallized from hexane. Yield: 25 g (45%), yellow prisms. Mp: 53−54 °C. Anal. Calcd for $C_{14}H_{18}O_3$: C, 71.8; H, 7.7. Found: C, 71.7; H, 7.7. MS (FAB): $m/z = 235$, $[M + H]^+$. ^{1}H NMR ($CDCl_3$): δ 1.38 (s, 9 H, *t*-bu), 2.72 (s, 6 H, COMe), 8.02 (s, 2 H, Ar), 13.11 (s, 1 H, OH).

2,6-Bis(acetoximato)-4-methylphenol (H_2Damox). A solution of NaOH (1.6 g, 40 mmol) in 15 mL of H_2O was added slowly to a refluxing solution of 2,6-diacetyl-4-methylphenol (1.92 g, 10 mmol) and hydroxylamine hydrochloride (3.1 g, 45 mmol) in 25 mL of ethanol. The solution was refluxed for 1 h and concentrated (rotary evaporator). The product was filtered off, recrystallized from aqueous ethanol, and dried over P_4O_{10}. Yield: 1.6 g (70%), white needles. Mp: 170 °C. Anal. Calcd for $C_{11}H_{14}N_2O_3$: C, 59.5; H, 6.4; N, 12.6. Found: C, 59.3; H, 6.3; N, 12.3. MS: $m/z = 222$, $[M^+]$. ^{1}H NMR (acetone-d_6): δ 1.55 (s, 3H, Ar−Me), 2.25 (s, 6 H, COMe), 7.17 (s, 2 H, Ar), 10.25 (s, 2 H, NOH), 11.70 (s, 1 H, Ar−OH).

2,6-Bis(acetoximato)-4-*tert*-butylphenol (H_2Dabox). This compound was synthesized using a procedure similar to that for H_2Damox. Yield: 85%, white needles. Mp: 150 °C. Anal. Calcd for $C_{14}H_{20}N_2O_3$: C, 63.6; H, 7.6; N, 10.6. Found: C, 63.3; H, 7.5; N, 10.8. MS (FAB): $m/z = 265$, $[M + H]^+$.

[Cu_2(Damox)$_2$] (1). A solution of 0.6 g (2.7 mmol) of H_2Damox in 15 mL of warm acetic acid was added to 0.65 g (3.2 mmol) of $Cu(CH_3COO)_2 \cdot H_2O$ in 15 mL of the same solvent. The green solution obtained was diluted to 200 mL with ethanol. After 5 days, the green-black prisms were filtered off, washed with ethanol, and dried over P_4O_{10} in vacuo. Yield: 0.63 g (82%). Anal. Calcd for $C_{22}H_{24}Cu_2N_4O_6$: C, 46.6; H, 4.2; N, 9.9; Cu, 22.4. Found: C, 46.6; H, 4.3; N, 9.8; Cu, 22.1. MS (FAB): $m/z = 567$, $[M]^+$.

[Ni_2(Damox)$_2$(MeOH)$_2$]·MeOH (2). A solution of $Ni(CH_3COO)_2 \cdot 4H_2O$ (0.5 g, 2 mmol) in 30 mL of warm MeOH was added to a stirred solution of H_2Damox (0.44 g, 2 mmol) in 50 mL of MeOH. The initially dark blue color changed to green in ∼5 min, and an apple-green precipitate formed. After 1 h the solid was filtered off, washed thoroughly with MeOH, and dried over $CaCl_2$ in vacuo. Yield: 0.52 g (80%). Anal. Calcd for $C_{25}H_{36}N_4Ni_2O_9$: C, 45.9; H, 5.5; N, 8.6. Found: C, 46.1; H, 5.4; N, 8.8.

[Ni_2(Damox)$_2$(Py)$_2$]·Py (3). Pink crystals were deposited when a saturated solution of **2** in warm pyridine was cooled. These were filtered off, washed with ether, and dried in vacuo over H_2SO_4. The crystals lose their luster upon desiccation. Anal. Calcd for $C_{37}H_{39}N_7Ni_2O_6$: C, 55.9; H, 4.9; N, 12.3. Found: C, 55.7; H, 4.8; N, 12.3.

[Cu_2(Damfb)] (4). Complex **1** (1.36 g, 2.4 mmol) was dissolved in the minimum volume of redistilled boron trifluoride ethyl etherate. The green solution was poured onto crushed ice, and the precipitate was filtered off, washed with water, recrystallized from acetone as greenish-black prisms, and air-dried. Anal. Calcd for acetone monosolvate: $C_{25}H_{28}B_2Cu_2F_4N_4O_7$: C, 41.7; H, 3.9; N, 7.8; Cu, 19.2. Found: C, 41.7; H, 4.2; N, 7.6. This was subsequently dried at 160 °C in vacuo to yield 1.0 g (70%) of the unsolvated green product. Anal. Calcd for $C_{22}H_{22}B_2Cu_2F_4N_4O_6$: C, 39.8; H, 3.3; N, 8.5; Cu, 19.2. Found: C, 39.8; H, 3.4; N, 8.4; Cu, 18.7. MS (FAB): $m/z = 663$, $[M + H]^+$.

[Cu_2(Dabox)$_2$] (5). A solution of $Cu(CH_3COO)_2 \cdot H_2O$ (0.4 g, 2 mmol) in 25 mL of MeOH was added to a MeOH solution (30 mL) of H_3L,[2] and the mixture was stirred for 3 h. The brownish green precipitate was filtered off, washed with MeOH and recrystallized from CH_2Cl_2−MeOH as olive green microcrystals. Yield: 0.42 g (65%). Anal. Calcd for $C_{28}H_{36}Cu_2N_4O_6$: C, 51.6; H, 5.5; N, 8.6. Found: C, 51.6; H, 5.5; N, 8.7. MS (FAB): $m/z = 651$, $[M + H]^+$.

[Ni_2(Dabox)$_2$(H_2O)$_2$] (6). This compound was synthesized in 75% yield from $Ni(CH_3COO)_2 \cdot 4H_2O$ and H_2Dabox using a procedure similar to that for **5**. Insolubility in common solvents prevented recrystallization. Anal. Calcd for $C_{28}H_{40}N_4Ni_2O_8$: C, 49.6; H, 5.9; N, 8.3. Found: C, 50.0; H, 5.7; N, 8.1.

[Cu_2(Dabfb)]·H_2O (7). Complex **5** (0.3 g) in redistilled $BF_3 \cdot Et_2O$ (10 mL) was heated on a steam bath for 15 min. The resulting dark green solid was filtered off, washed with ether, and recrystallized from CH_3CN−MeOH. Yield: 0.25 g (70%). Anal. Calcd for $C_{28}H_{36}B_2Cu_2F_4N_4O_7$: C, 43.9; H, 4.7; N, 7.3. Found: C, 43.6; H, 4.7; N, 7.2. MS (FAB): $m/z = 747$, $[M + H]^+$.

[Ni_2(Dabfb)] (8). Using the same procedure as for **7**, this compound was synthesized from **6** and recrystallized from CH_2Cl_2−toluene as dark red crystals in 65% yield. Anal. Calcd for $C_{28}H_{34}B_2F_4N_4Ni_2O_6$: C, 45.6; H, 4.6; N, 7.6. Found: C, 45.4; H, 4.7; N, 7.7. MS (FAB): $m/z = 717$, $[M - F]^+$. ^{1}H NMR ($CDCl_3$): δ 1.30 (s, 9 H, *t*-Bu), 2.32 (s, 6 H, Me), 7.37 (s, 2 H, Ar).

The cationic macrocyclic chelates $[Cu_2(Dampn)]^{2+}$ and $[Cu_2(Dambn)]^{2+}$ were prepared by addition of 1,3-diaminopropane (0.78 g, 10.5 mmol) or 1,4-diaminobutane (0.92 g, 10.5 mmol), respectively,

(17) Rosenmund, K. W.; Schulz, H. *Arch. Pharm. (Weinheim, Ger.)* **1927**, *265*, 308.

to copper(II) acetate (2.0 g, 10 mmol) in 20 mL ethanol, followed by sodium acetate (ca. 4 g, 50 mmol) and diacetylcresol (1.92 g, 10 mmol) in 10 mL of ethanol. After 10 h of reflux, the ethanol was (rotary) evaporated off and replaced by water. The green complexes were precipitated by addition of $NaNO_3$, and the nitrate salts, recrystallized from water and air-dried, were quantitatively metathesizable in aqueous methanol into the ClO_4^- or $CF_3SO_3^-$ salts, which were dried over P_4O_{10}. The nitrates release water of crystallization when desiccated, yielding hygroscopic products.

$[Cu_2(Dampn)](NO_3)_2 \cdot 4H_2O$ (9) (Green Prisms). Anal. Calcd for $C_{28}H_{34}Cu_2N_6O_8 \cdot 4H_2O$: C, 44.8; H, 5.44; N, 10.8; Cu, 16.3. Found: C, 44.4; H, 4.98; N, 10.8; Cu, 16.2. MS (FAB): $m/z = 584$, $[M - 2NO_3]^+$.

$[Cu_2(Dampn)](ClO_4)_2$ (10) (Green Needles). Anal. Calcd for $C_{28}H_{34}Cl_2Cu_2N_4O_{10}$: C, 42.8; H, 4.37; N, 7.14; Cu, 16.2. Found: C, 42.4; H, 4.46; N, 6.83; Cu, 16.2. MS (FAB): $m/z = 584$, $[M - 2ClO_4]^+$.

$[Cu_2(Dambn)](NO_3)_2 \cdot 2H_2O$ (11) (Green Crystals). Anal. Calcd for $C_{30}H_{38}Cu_2N_6O_8 \cdot 2H_2O$: C, 46.7; H, 5.43; N, 10.9; Cu, 16.4. Found: C, 46.7; H, 5.51; N, 10.6; Cu, 16.4. MS (FAB): $m/z = 613$, $[M - 2NO_3]^+$.

$[Cu_2(Dambn)](ClO_4)_2 \cdot CH_3OH$ (12). Anal. Calcd for $C_{31}H_{42}Cl_2Cu_2N_4O_{11}$: C, 44.1; H, 5.01; N, 6.63; Cu, 15.0. Found: C, 44.0; H, 4.95; N, 6.60; Cu, 14.6. MS (FAB): $m/z = 713$, $[M - ClO_4]^+$

$[Cu_2(Dambn)](CF_3SO_3)_2$ (13) (Green Powder). Anal. Calcd for $C_{32}H_{38}Cu_2F_6N_4O_8S_2$: C, 42.2; H, 4.17; N, 6.15. Found: C, 42.5; H, 4.28; N, 5.88. MS (FAB): $m/z = 763$, $[M - CF_3SO_3]^+$.

[Cu(Apmpn)] (14). This neutral Schiff base chelate, a mononuclear analogue of $[Cu_2(Dampn)]^{2+}$, was prepared by refluxing $Cu(OAc)_2 \cdot H_2O$ (5 mmol) with the stoichiometric amounts of *o*-hydroxyacetophenone, 1,3-diaminopropane (2:1), and NEt_3 (10 mmol) in MeOH (40 mL) for 2 h. The precipitate was recrystallized from MeCN and dried in vacuo over P_4O_{10} to give 1.2 g (3 mmol, 60%) of deep green prisms. Anal. Calcd for $C_{19}H_{20}CuN_2O_2$: C, 61.4; H, 5.42; N, 7.53. Found: C, 61.6; H, 5.57; N, 7.58.

Physical Measurements. Infrared spectra were recorded on a Perkin-Elmer 1610 FT-IR using KBr disks. EPR spectra were obtained with a Varian E-12 X-band spectrometer calibrated near $g = 2$ with diphenylpicrylhydrazyl radical. *g*-values are ± 0.005 ($g_{||}$) and ± 0.01 ($g_\perp$); isotropic *g*-values (± 0.005) are designated g_o. Electronic spectra are from a Perkin-Elmer 330 spectrophotometer, equipped with an integrating sphere for diffuse reflectance. Mass spectra were obtained either on a Finnigan-4500 or a ZABHF mass spectrometer. ^1H NMR spectra were obtained on a Bruker AC 250 spectrometer using $CDCl_3$ or acetone-d_6 solutions with TMS as the internal standard. Variable-temperature magnetic susceptibility data were collected in the range 4−300 K by using an Oxford Instruments superconducting Faraday magnetic susceptibility system with a Sartorius 4432 microbalance. A main solenoid field of 1.5 T and a gradient field of 10 T m^{-1} were employed. Susceptibility data were corrected for diamagnetism using Pascal's constants. $HgCo(NCS)_4$ was used as a calibration standard. Data were analyzed using SAS Institute's JMP-3.1 or MathSoft's MathCad Plus-6 least-squares procedures on a Macintosh 603e platform. Electrochemical measurements were made at 25 °C in deoxygenated CH_3CN, pyridine, or DMF solutions using a BAS 100A electrochemical analyzer or a PAR-173/175/176 system incorporating an MPI MP-1012 integrator. The three-electrode assembly comprised the working electrode, an Ag^+ (0.01 M, 0.1 M NEt_4ClO_4, CH_3CN)/Ag reference electrode, and a Pt auxiliary electrode. The working electrodes were Pt disk, beads, or wires for voltammetry at scan rates from 20 to 2000 mV s^{-1} and a Pt disk for rotating electrode (rde) polarography (wherein the $E_{1/2}$'s are defined as the potential at which $i = i_L/2$). The supporting electrolyte was 0.1−0.2 M NEt_4ClO_4, and solutions for voltammetry and polarography were ca. 1 mM in complex. Coulometry was performed on analytes at the 10^{-2} M level at a Pt-gauze electrode with the Pt counter electrode separated in a compartment of permeable Vycor.

X-ray Crystallography. Single crystals of $[Ni_2(Damox)_2(Py)_4] \cdot 2Py$ (**3a**) were obtained from a saturated solution of $[Ni_2(Damox)_2(MeOH)_2] \cdot MeOH$ (**2**) in pyridine. These crystals are unstable when dry, so the one used for the X-ray crystallographic study was sealed in a capillary tube with mother liquor. Single crystals of $[Ni_2(Dabfb)]$ (**8**) were obtained by diffusing ether into a 1,1,2,2-tetrachloroethane solution of the complex.

Table 1. Crystallographic Data for $[Ni_2(Damox)_2(Py)_4] \cdot 2Py$ (**3a**) and $[Ni_2(Dabfb)]$ (**8**)

	3a	**8**
formula	$C_{52}H_{54}N_{10}O_6Ni_2$	$C_{28}H_{34}B_2F_4N_4O_6Ni_2$
fw	1032.5	737.6
cryst system	monoclinic	orthorhombic
cryst size, mm	0.42 × 0.40 × 0.23	0.40 × 0.10 × 0.10
space group	$P2_1/n$	*Pnma*
a, Å	13.297(5)	11.558(6)
b, Å	11.240(5)	17.200(5)
c, Å	17.396(6)	16.058(2)
β, deg	109.03(3)	90
V, Å^3	2458(3)	3192(3)
Z	2	4
D_{calc}, g cm^{-3}	1.39	1.54
F(000)	1076	1520
μ, cm^{-1}	8.27	12.53
λ(Mo Kα), Å	0.710 69	0.710 69
T, K	293	293
R,[a] R_w[b]	0.050, 0.052	0.057, 0.057

[a] $R = \sum||F_o| - |F_c||/\sum|F_o|$. [a] $R_w = [\sum w(|F_o| - |F_c|)^2/\sum w(F_o)^2]^{1/2}$.

All measurements were made as previously described[18] on a Rigaku AFC6S diffractometer with graphite-monochromated Mo Kα radiation. Pertinent crystallographic data are summarized in Table 1. Cell constants and an orientation matrix for data collection were obtained from a least-squares refinement of setting angles of 25 reflections. The intensities of three standard reflections measured after every 150 reflections showed no greater fluctuations than expected from Poisson statistics. Lorentz−polarization and absorption corrections were applied. A total of 6079 and 7135 reflections were collected for $[Ni_2(Damox)_2(Py)_4] \cdot 2Py$ (**3a**) and $[Ni_2(Dabfb)]$ (**8**), respectively, of which 5400 ($R_{int} = 0.152$) and 3568 ($R_{int} = 0.110$) were unique; equivalent reflections were averaged. Of these, 2494 reflections for **3a** and 1374 reflections for **8** had $F_o^2 > 3\sigma_{F_o^2}$, where $3\sigma_{F_o^2}$ was estimated from counting statistics.[18,19]

The metal atoms were located from 3-D Patterson maps and the rest of the non-hydrogen atoms emerged from successive Fourier synthesis. In the case of $[Ni_2(Damox)_2(Py)_4] \cdot 2Py$ (**3a**), 6-fold positional disorder around the pyridine hexagon in the pyridine molecules of solvation makes the six sites equivalent so that each of the H-locations in the hexagon corresponds to $^5/_6$ of a full H. In $[Ni_2(Dabfb)]$ (**8**), the molecule lies on a symmetry plane with the two halves on either side of the O(1)−O(2) line of bridging oxygens. One of the two *tert*-butyl groups in **8** exhibits rotational disorder. The structures were refined by full-matrix least-squares methods using the TEXRAY[20] program set. Neutral atom scattering factors were taken from Cromer and Waber.[21] All the non-hydrogen atoms were refined anisotropically except for the disordered *tert*-butyl carbons, while the hydrogen atoms were placed at the geometrically calculated positions with fixed isotropic thermal parameters. The highest residues were 0.38 e Å^{-3} (**3a**) and 0.54 e Å^{-3} (**8**). Atomic coordinates for the most important atoms of **3a** and **8** are given in Tables 2 and 3, respectively.

Results and Discussion

Synthesis. The oximes of the diacetyl phenols (H_2Damox and H_2Dabox) are prepared in good yields via their reaction with excess NH_2OH. H_2Damox is a photosensitive compound. The dicopper(II) complex, $[Cu_2(Damox)_2]$ (**1**), is stable enough to be prepared in glacial acetic acid using equivalent amounts

(18) Backhouse, J. R.; Lowe, H. M.; Sinn, E.; Suzuki, S.; Woodward, S. *J. Chem. Soc., Dalton Trans.* **1995**, 1489.
(19) Corfield, P. W. P.; Doedens, R. J.; Ibers, J. A. *Inorg. Chem.* **1967**, *6*, 197.
(20) *TEXSAN-TEXRAY Structure Analysis Package*; Molecular Structure Corp: The Woodlands, TX, 1985.
(21) Cromer, D. T.; Waber, J. T. *International Tables for X-ray Crystallography*; The Kynoch Press: Birmingham, England, 1974; Vol. IV.

Table 2. Positional Parameters for Selected Atoms of $[Ni_2(Damox)_2(Py)_4]\cdot 2Py$ (**3a**)

atom	*x*	*y*	*z*
Ni	−0.07599(7)	−0.10621(7)	−0.01774(5)
O(1)	−0.0806(3)	0.0725(3)	0.0018(2)
O(2)	−0.2839(4)	−0.2140(4)	−0.0614(3)
O(3)	0.1399(4)	0.3463(4)	0.0594(3)
N(1)	−0.0404(4)	−0.1457(4)	0.1095(3)
N(2)	0.0501(4)	0.2777(4)	0.0399(3)
N(3)	−0.2354(4)	−0.1074(5)	−0.0363(3)
N(4)	−0.1278(4)	−0.0816(4)	−0.1544(3)
C(1)	−0.1564(5)	0.1448(5)	0.0052(3)
C(2)	−0.2642(5)	0.1022(6)	−0.0154(3)
C(6)	−0.1369(5)	0.2675(5)	0.0278(3)
C(8)	−0.2998(5)	−0.0189(6)	−0.0403(4)
C(10)	−0.0327(5)	0.3274(5)	0.0505(4)
N(41)[a]	−0.178(2)	0.259(2)	0.379(1)

[a] Occupancy 0.420.

Table 3. Positional Parameters for Selected Atoms of $[Ni_2(Dabfb)]$ (**8**)

atom	*x*	*y*	*z*	occ
Ni	0.18314(8)	0.16771(5)	0.04537(6)	
O(1)	0.2673(6)	1/4	0.0001(5)	1/2
O(2)	0.0984(6)	1/4	0.0883(5)	1/2
O(3)	0.3011(5)	0.0244(3)	0.0321(4)	
O(4)	0.1308(5)	0.0233(3)	0.1155(4)	
N(1)	0.2810(6)	0.0962(3)	−0.0059(5)	
N(2)	0.0866(6)	0.0946(4)	0.0962(4)	
B	0.257(1)	0.0191(7)	0.1183(8)	
C(1)	0.306(1)	1/4	−0.0778(8)	1/2
C(2)	0.3326(6)	0.1798(4)	−0.1180(5)	
C(5)	0.3361(7)	0.1050(5)	−0.0756(6)	
C(11)	−0.019(1)	1/4	0.0994(6)	1/2
C(12)	−0.0778(6)	0.1799(5)	0.1071(5)	
C(15)	−0.0216(7)	0.1044(5)	0.1159(5)	

of H_2Damox and $Cu(CH_3COO)_2\cdot H_2O$. This compound is insoluble in common organic solvents, but obtained as pure microcrystals by diluting the reaction mixture with EtOH. All the other dicopper(II) and dinickel(II) complexes of the oximes were obtained from the reaction of the corresponding oxime and metal(II) acetate in MeOH. Pyridine solutions of $[Ni_2(Damox)_2(MeOH)_2]\cdot$MeOH (**2**) afford pink crystals of $[Ni_2(Damox)_2(Py)_4]\cdot 2Py$ (**3a**). These crystals effloresce coordinated as well as solvent of crystallization pyridine molecules to form $[Ni_2(Damox)_2(Py)_2]\cdot$Py (**3**). For comparative purposes, a copper(II) N_2O_2 chelate was prepared from the mononucleating Schiff base ligand ($ApmpnH_2$) prepared from condensing 1,3-diaminopropane in 1:2 ratio with the singly acetylated phenol, *o*-hydroxyacetophenone. Macrocyclization of the dioximato complexes was effected by treating them with boron trifluoride ethyl etherate.[22] In the case of $[Ni_2(Damox)_2(MeOH)_2]\cdot$MeOH (**2**), we were unable to isolate the pure BF_2-bridged macrocyclic complex. Compounds of the $M_2(Damox)_2$ type are relatively insoluble in most common solvents unless they are strongly coordinating (such as pyridine). Although this insolubility can be significantly ameliorated by using the *tert*-butyl rather than the methyl derivatives, some difficulties remained for solution studies.

Electronic Spectra. The electronic spectral data for the complexes are summarized in Table 4. The spectrum of $[Ni_2(Damox)_2(Py)_4]\cdot 2Py$, generated by dissolving $[Ni_2(Damox)_2(Py)_2]\cdot$Py in pyridine, exhibits three d−d bands at 900, 595, and 470 nm. These are attributed in an octahedral model to the transitions $^3A_{2g} \rightarrow {}^3T_{2g}$, $^3A_{2g} \rightarrow {}^3T_{1g}$, and $^3A_{2g} \rightarrow {}^3T_{1g}(P)$.[23] Furthermore, the spectrum of $[Ni_2(Damox)_2(Py)_2]\cdot$Py (**3**) in the solid state is similar to that of solid $[Ni_2(Damox)_2(MeOH)_2]\cdot$MeOH (**2**) and solid $[Ni_2(Dabox)_2(H_2O)_2]$ (**6**), for which six-coordination is implausible. The bands observed are of energy similar to those of other well-characterized square-pyramidal high-spin nickel(II) complexes,[1,23,24] while $[Ni_2(Dabfb)]$ (**8**) in CH_2Cl_2 solution exhibits a single intense d−d band at 540 nm, characteristic of diamagnetic square-planar nickel(II) complexes.[25,26] This complex's unexpected resistance to adopting hexacoordination is evidenced by its optical spectrum in neat γ-picoline, which again appears to be that of a pentacoordinate nickel system rather than of a tetrakis(picoline) adduct.

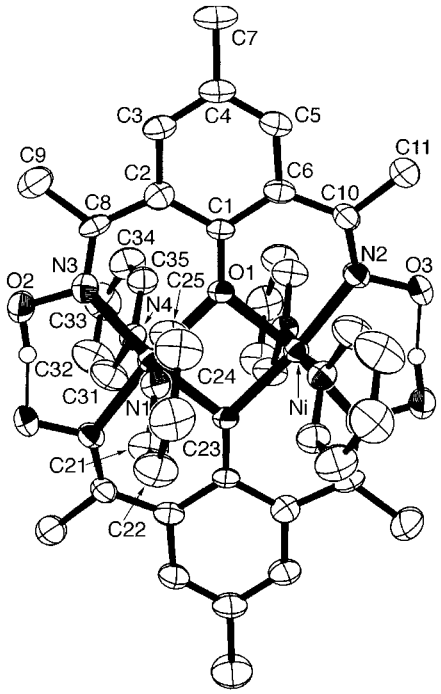

Figure 1. ORTEP representation (H's omitted for clarity of presentation) of $[Ni_2(Damox)_2(Py)_4]$ in $[Ni_2(Damox)_2(Py)_4]\cdot(Py)_2$ (**3a**).

All of the copper(II) complexes show a d−d transition around 600 nm, which is typical of square-planar N_2O_2-ligated copper(II), and a shoulder in the 405−435 nm range which can be assigned to O^-(phenolate) → Cu(II) charge transfer.[27] Intense absorption in the ultraviolet region is a feature common to all the copper(II) and nickel(II) complexes and is attributed to intraligand charge-transfer transition.

Description of the Structure of $[Ni_2(Damox)_2(Py)_4]\cdot(Py)_2$ (3a). The ORTEP representation of **3a** is given in Figure 1, and interatomic distances and angles relevant to the coordination sphere are given in Table 5. The centrosymmetric structure contains two nickel centers bridged by two phenoxide oxygen atoms with two imine nitrogen donors completing the NiN_2O_2 equatorial plane. The center of inversion is between the two nickel ions. Each of the metal centers achieves a pseudo-octahedral configuration through the axial coordination of

(22) Addison, A. W.; Carpenter, M.; Lau, L. K.-M.; Wicholas, M. *Inorg. Chem.* **1978**, *17*, 1545: CO-binding constant estimates from $K^I = (1/a_{CO})(e^{0.03892\Delta E} - 1)$, ΔE in mV.

(23) Lever, A. B. P. *Inorganic Electronic Spectroscopy*, 2nd ed.; Elsevier: New York, 1984.

(24) Nanda, K. K.; Das, R.; Newlands, M. J.; Hynes, R.; Gabe, E. J.; Nag, K. *J. Chem. Soc., Dalton Trans*. **1992**, 897.

(25) Streeky, J. A.; Pillsbury, D. G.; Busch, D. H. *Inorg. Chem.* **1980**, *19*, 3148

(26) Nanda, K. K.; Das, R.; Venkatsubramanian, K.; Paul, P.; Nag, K. *J. Chem. Soc., Dalton Trans*. **1993**, 2515.

(27) Amundsen, A. R.; Whelan, J.; Bosnich, B. *J. Am. Chem. Soc*. **1977**, *99*, 6730.

Table 4. Electronic Spectral[a] Data for the Complexes

complex	medium	λ_{max}, nm (ϵ, M^{-1} cm^{-1})
$[Cu_2(Damox)_2]$ (**1**)	solid state	620, 430 (sh), 370 (sh)
$[Cu_2(Damox)_2]$	pyridine	625 (650), 355 (15 900), 307 (19 300)
$[Ni_2(Damox)_2(MeOH)_2]\cdot MeOH$ (**2**)	solid state	1250 (br), 1000 (br), 600, 410 (sh), 360
$[Ni_2(Damox)_2(Py)_2]\cdot Py$ (**3**)	solid state	1600, 980, 625, 470 (sh), 380
$[Ni_2(Damox)_2(Py)_2]\cdot Py$	pyridine	900 (20), 595 (52), 470 (180)
$[Cu_2(Damfb)]$ (**4**)	CH_2Cl_2	600 (125, sh), 405 (1,070, sh),
$[Cu_2(Damfb)]$		340 (11 200)
$[Cu_2(Damfb)]$	acetone	610 (100), 344 (12,100)
$[Cu_2(Damfb)]$	pyridine	635 (390), 353 (11 300), 305 (5900)
$[Cu_2(Dabox)_2]$ (**5**)	DMF	598 (290), 420 (1,700, sh), 348 (14 200)
$[Ni_2(Dabox)_2(H_2O)_2]$ (**6**)	solid state	1175, 600 (br), 430 (sh), 345 (sh)
$[Cu_2(Dabfb)]\cdot H_2O$ (**7**)	CH_2Cl_2	615 (135, sh), 435 (1,360, sh), 390 (11 400)
$[Ni_2(Dabfb)]$ (**8**)	CH_2Cl_2	540 (320), 348 (7,750)
$[Ni_2(Dabfb)]$	DMF	1060 (87), 495 (sh, 114), 355 (9830)
$[Ni_2(Dabfb)]$	γ-picoline	1570 (34), 855 (18), 800 (16, sh), 585 (52), 360 (9820)
$[Cu_2(Dampn)](NO_3)_2\cdot 4H_2O$ (**9**)	MeOH	575 (156), 352 (16 200)
$[Cu_2(Dampn)](NO_3)_2\cdot 4H_2O$	pyridine	590 (370), 358 (13 300), 305 (4,100)
$[Cu_2(Dambn)](NO_3)_2\cdot 2H_2O$ (**11**)	MeOH	625 (116), 350 (15 200)
$[Cu_2(Dambn)](NO_3)_2\cdot 2H_2O$	pyridine	625 (500), 360 (9000), 305 (7200)
[Cu(Apmpn)] (**14**)	CH_3CN	580 (265), 360 (11 000)

[a] Solid-state data from diffuse reflectance in $MgCO_3$ matrix.

Table 5. Selected Interatomic Distances (Å) and Angles (deg) for $[Ni_2(Damox)_2(Py)_4]\cdot 2Py$ (**3a**)

Ni···Ni′	3.058(2)	Ni−O(1)	2.042(4)
Ni−N(1)	2.154(5)	Ni−N(2)	2.017(5)
Ni−N(3)	2.038(6)	Ni−N(4)	2.265(5)
O(1)−Ni−O(1)	83.1(2)	O(1)−Ni−N(1)	92.3(2)
O(1)−Ni−N(2)	171.2(2)	O(1)−Ni−N(3)	87.0(2)
O(1)−Ni−N(4)	92.2(2)	O(1)−Ni−N(1)	91.5(2)
O(1)−Ni−N(2)	88.5(2)	O(1)−Ni−N(3)	169.7(2)
O(1)−Ni−N(4)	93.9(2)	N(1)−Ni−N(2)	90.3(2)
N(1)−Ni−N(3)	91.7(2)	N(1)−Ni−N(4)	173.4(2)
N(2)−Ni−N(3)	101.4(2)	N(2)−Ni−N(4)	85.9(2)
Ni−O(1)−Ni	96.9(2)	N(3)−Ni−N(4)	83.7(2)

pyridine nitrogens. The two nickel atoms are separated by 3.058 Å with a Ni−O−Ni bridge angle of 96.9°. On each nickel, the two Ni−N(pyridine) bonds are, however, not equal (Ni−N(1) = 2.154 and Ni−N(4) = 2.265 Å). The pyridine rings on the same side of the metals' equatorial plane are almost parallel (the rings are inclined at 12.5° to each other) and are separated by approximately 3.5 Å. This π-interaction is probably responsible for the stability of the octahedral tetrapyridine adduct in pyridine solution and in the solid state under a sensible pyridine vapor pressure. The apparent equivalence of the two nickels in $Ni_2(Damox)_2(Py)_3$ indicates that the hexapyridine adduct loses two coordinated pyridine molecules and a pyridine of solvation in the absence of pyridine vapor and forms square-pyramidal $[Ni_2(Damox)_2(Py)_2]\cdot Py$ (**3**). Strong H-bonding between oxime-H's and oximato-O's renders the structure pseudomacrocyclic.

Description of the Structure of $[Ni_2(Dabfb)]$ (8). The molecule consists of a neutral binuclear nickel(II) complex with no close intermolecular contacts. The asymmetric unit consists of half the molecule, the other half being mirrored in a plane that bisects the O(1)−O(2) line of the bridging phenoxide oxygen atoms. The ORTEP representation of **8** with the atom-numbering scheme is given in Figure 2a, and interatomic distances and angles relevant to the nickel coordination sphere are in Table 6. The molecular diagram in Figure 2b shows the marked saddle-shaped bending of the macrocyclic ligand. This dramatic curvature puts the boron atoms a full 1.45 Å above the NiN_2O_2 center. Molecular models indicate that diimine end caps on the dimetallic bis(diimino−phenolate) moiety would be essentially planar if these diimine ends were closed off as

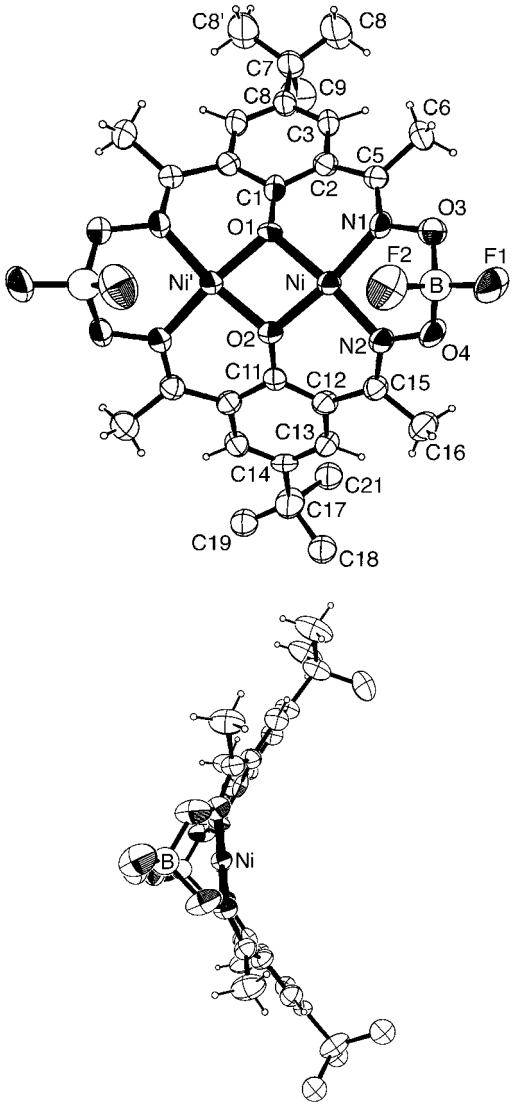

Figure 2. (a) Top: ORTEP diagram and atom-labeling scheme of $[Ni_2(Dabfb)]$ (**8**) (H's omitted for clarity). (b) Bottom: Perspective view showing the saddle shape of the molecule.

five-membered rings. However, construction of the six-membered ring ($NiBN_2O_2$) forces out of the plane the only ring

Table 6. Selected Interatomic Distances (Å) and Angles (deg) for $[Ni_2(Dabfb)]$ (**8**)

Ni···Ni′	2.831(2)	Ni−O(1)	1.865(5)
O(2)−C(11)	1.36(1)	Ni−O(2)	1.854(5)
O(3)−N(1)	1.396(7)	Ni−N(1)	1.863(7)
Ni−N(2)	1.869(6)	O(4)−N(2)	1.364(7)
O(3)−B	1.48(1)	O(4)−B	1.46(1)
F(1)−B	1.35(1)	F(2)−B	1.38(1)
O(1)−Ni−O(2)	80.9(2)	N(2)−O(4)−B	115.2(7)
O(1)−Ni−N(1)	90.7(3)	Ni−N(1)−O(3)	119.5(5)
O(1)−Ni−N(2)	172.9(3)	O(3)−N(1)−C(5)	113.5(6)
O(2)−Ni−N(1)	171.6(3)	Ni−N(2)−O(4)	118.7(5)
O(2)−Ni−N(2)	92.1(3)	N(1)−Ni−N(2)	96.4(3)
F(1)−B−F(2)	114(1)	Ni−O(1)−Ni′	98.7(3)
F(1)−B−O(3)	106.0(8)	Ni−O(2)−Ni′	99.5(3)
F(1)−B−O(4)	108.4(9)	F(2)−B−O(3)	109.6(9)
F(2)−B−O(4)	110.1(9)	N(1)−O(3)−B	113.9(7)
O(3)−B−O(4)	108.2(9)		

Table 7. Electrochemical[a] Data for the Complexes

		$E_{1/2}$[b]		
complex	medium	$M^{II}M^{II}/M^{II}M^{I}$	$M^{II}M^{I}/M^{I}M^{I}$	$10^8 D\eta$[c]
$[Cu_2(Damox)_2]$ (**1**)	DMF	−1.22 (q)	−1.58 (i)[d]	1.1
$[Cu_2(Damox)_2]$ (**1**)	DMF/CO	−1.16 (q)[e]	−1.71 (i)[f]	1.1
$[Cu_2(Damox)_2]$ (**1**)	Pyridine	−1.17 (q)	−1.72 (i)	2.4
$[Cu_2(Damfb)]$ (**4**)	DMF	−0.94 (q)	−1.45 (q)	1.5
$[Cu_2(Dabox)_2]$ (**5**)	DMF	−1.24 (q)	−1.68 (q)	1.8
$[Cu_2(Dabfb)]\cdot H_2O$ (**7**)	DMF	−0.93 (q)	−1.45 (q)	1.8
$[Ni_2(Dabfb)]$ (**8**)	CH_3CN	−1.15 (q)	−1.54 (q)	1.8
$[Cu_2(Dampn)](ClO_4)_2$ (**10**)	DMF	−0.96 (q)	*g,h*	1.0
$[Cu_2(Dampn)](ClO_4)_2$ (**10**)	DMF/CO	−0.88 (i)[f]	*g*	1.0
$[Cu_2(Dampn)](ClO_4)_2$ (**10**)	$MeNO_2$	−0.80[f]	−1.13[f]	3.3
$[Cu_2(Dambn)](ClO_4)_2$ (**12**)	DMF	−0.80 (q)	−1.17 (i)	1.3
$[Cu_2(Dambn)](CF_3SO_3)_2$ (**13**)	DMF	−0.78 (r)	−1.17 (q)	1.6
$[Cu_2(Dambn)](CF_3SO_3)_2$ (**13**)	DMF/CO	−0.72 (r)	−1.07 (q)	1.6
[Cu(Apmpn)] (**14**)	CH_3CN	−1.43 (i)		1.1

[a] $E_{1/2}$ in V vs Ag^+ (0.01 M, 0.1 M NEt_4ClO_4, CH_3CN)/Ag with Pt electrode, scan rate 0.1 V s^{-1}. This electrode is at ca. +0.545 V vs the SHE. [b] Key: i, irreversible ($E_{p,c}$); q, quasireversible (mean of $E_{p,c}$, $E_{p,a}$); r, reversible. [c] $D\eta$ in g cm s^{-2}, not adjusted for α, Ψ.[36] [d] $E_{1/2}$ values are −1.23 and −1.59 V in rde polarogram. H_2Damox itself has an irreversible reduction with $E_{1/2} = -2.22$ V in MeCN. [e] $E_{pc} = -1.175$ V. [f] $E_{1/2}$ values in rde polarogram. [g] Poorly defined wave at $E_{1/2} = -1.35$ V in rde polarogram. [h] −1.66 V in MeCN.

atom (B) not attached to the obligatorily trigonal nitrogens. The Schiff base ligand planes O(1)−C(1)−C(2)−C(5)−N(1) and O(2)−C(11)−C(12)−C(15)−N(2) make angles of 32.4 and 27.7°, respectively, with the Ni_2O_2 plane and 59.4° with each other. The phenyl rings C(1)−C(12)−C(13)−C(14)−C(13′)−C(14′) are at 36.1 and 32.3°, respectively with the NiN_2O_2 center and 68.4° with each other. On the other hand, the first coordination sphere about the nickel atoms is planar within 1°, and the ^{1}H-NMR confirms the $S = 0$ nature of the nickel ions.

Redox Properties. The compounds are readily reducible from the $M^{II}M^{II}$ to the $M^{I}M^{II}$ level (Table 7), as exemplified in Figure 3, and in all but a few cases this process is at least quasireversible on the voltammetry time scale, the ΔE_p values being 15−90 mV greater than those for a Nernstian standard under the same conditions. (The following discussion assumes that $k_r \simeq k_f$ ($\equiv k_o$) for the quasireversible processes.) The sequential nature of the reductions

$$M^{II}M^{II} + e^- \rightarrow M^{II}M^{I} \qquad E_1$$

$$M^{II}M^{I} + e^- \rightarrow M^{I}M^{I} \qquad E_2$$

in such bis(μ-phenoxo) systems has been explored

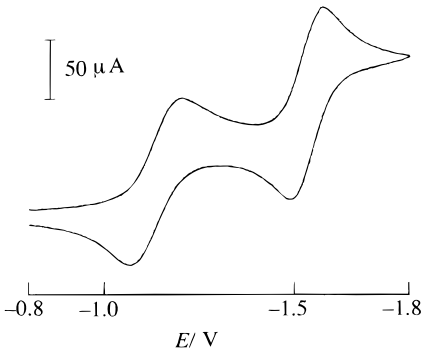

Figure 3. Cyclic voltammogram of $[Ni_2(Dabfb)]$ in CH_3CN with Pt working and auxiliary electrodes and Ag^+ (0.01 M, 0.1 M NEt_4ClO_4, CH_3CN)/Ag reference electrode at a scan rate of 100 mV s^{-1}.

previously,[2,28−30] and the normally substantial separation ($E_1 - E_2$) had generally been considered to be dominated by Coulombic effects,[28,29] though later work[31] has called this proposition into doubt. Nonetheless, simple extrapolation of the $E_1 - E_2$ values for dinuclear ruthenium(III/II) systems[32,33] with 5−11 Å Ru−Ru separations to the 2.85 Å Cu−Cu distances in the present compounds[34] leads to an $E_1 - E_2$ of 220−320 mV. In addition, a naive estimate for the change in Coulombic work for electron addition to a binuclear center:[35]

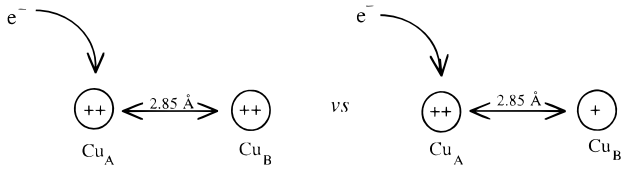

yields a value of 340 mV for the change in $E_{1/2}$ of Cu_A due to the change in Coulombic potential associated with Cu_B. Electrostatic effects are also consistent with the lowered $E_{1/2}$ seen for [Cu(Apmpn)], the uncharged mononuclear analogue of $[Cu_2(Dampn)]^{2+}$. These approaches support the contention that the electrostatic factor is a major if not the dominant component of $E_1 - E_2$.

Analysis of the appropriate current functions[36−38] for the compounds indeed yielded $D\eta$ values ($(1-3) \times 10^{-8}$, Table 7) consistent with $n = 1$ processes,[39] and this was confirmed in the case of $[Cu_2(Dambn)](ClO_4)_2$ by its $n = 2$ coulometry in DMF/NEt_4ClO_4 at − 1.5 V at a Pt-mesh cathode, the *i:Q* plot[40] for 100 μmol of which extrapolated to 210 μF at $t = \infty$. The reduced nickel chelates do not all possess long-term stability,

(28) Gagné, R. R.; Koval, C. A.; Smith, T. J.; Cimolino, M. C. *J. Am. Chem. Soc.* **1979**, *101*, 4571.
(29) Long, R. C.; Hendrickson, D. N. *J. Am. Chem. Soc.* **1983**, *105*, 1513.
(30) Mandal, S. K.; Nag, K. *J. Chem. Soc., Dalton Trans.* **1983**, 2429.
(31) Mandal, S. K.; Adhikary, B.; Nag, K. *J. Chem. Soc., Dalton Trans.* **1986**, 1175.
(32) Goldsby, K. A.; Meyer, T. J. *Inorg. Chem.* **1984**, *23*, 3002.
(33) Sutton, J. E.; Sutton, P. M.; Taube, H. *Inorg. Chem.* **1979**, *18*, 1017.
(34) Carlisle, W. D.; Fenton, D. E.; Roberts, P. B.; Casellato, U.; Vigato, P. A.; Graziani, R. *Trans. Met. Chem. (Weinheim)* **1986**, *11*, 292.
(35) Using $E = (Nq_e/4\pi\epsilon)((q_A/x) + (q_B/d))$, adopting a value of $35\epsilon_o$ for the dielectric (typical of DMF, MeCN, and $MeNO_2$) and a value of +4.35 V for the absolute potential of the SHE, and thus setting $d =$ 2.85 Å and $x = 0.23$ Å to match an E_1 of −0.45 V vs SHE.
(36) Nicholson, R. S.; Shain, I. *Anal. Chem.* **1964**, *36*, 706.
(37) Piekarski, S.; Adams, R. N. in *Techniques of Chemistry*, Weissberger, A., Rossiter, B. W., Eds.; Wiley-Interscience: New York, 1971; Vol. 1, Part IIA, p 541.
(38) (a) Stephens, M. M.; Moorhead, E. D. *J. Electroanal. Chem.* **1984**, *164*, 17. (b) Varadharajan, U.; Butcher, R. J.; Kanters, R. F. P.; Addison, A. W.; Jasinski, J. P. Submitted for publication.

as evidenced by significantly less than unity values for i_{pa},i_{pc}, for example for [Ni_2(Dabfb)]. Indeed, a butyronitrile/NEt_4ClO_4 solution in which [Ni_2(Dabfb)]$^-$ had been cathodically electrogenerated yielded no EPR signal at 77 K. Similarly, the fully reduced [Cu^I_2(Dabox)$_2$]$^{2-}$ is not stable in DMF while [Cu^I_2(Damox)$_2$]$^{2-}$ and [Cu^I_2(Dambn)]^0 are unstable in pyridine, as revealed by the irreversible voltammograms ($\Delta E_{p,corr} > 70$ mV, i_{pa},$i_{pc} \ll 1$) for their generation (Table 7). The oxidative electrochemistry is also generally irreversible, as typically represented by an $n = 1$ wave at +0.65 V in the rde polarogram of Cu_2(Damox) and an oxidation at ca. +1.5 V for [Ni_2(Dabfb)]. However, some interactions of the reduced species with carbon monoxide were observable in DMF solution; the carbonyl formed by the 2,6-diformyl-4-methylphenol-derived analogue of [Cu_2(Dampn)]$^{+/0}$ has been examined previously in MeCN by Gagné *et al.*[28,41] We were initially surprised to see that in DMF under 1 atm of CO the reversible E_1 process for the copper complex of the quite basic ligand Damox becomes completely irreversible (i_{pa},$i_{pc} \ll 1$). The same is true for [Cu_2(Damfb)] and [Cu_2(Dampn)]$^{2+}$. On the other hand, for [Cu_2(Dambn)]$^{2+}$ both voltammetric waves move to more anodic potential under CO and their reversibility is not significantly affected (Table 7). The concomitant shifts enable estimation[22] of these rather weak copper(I)−CO binding constants as $K^I_{A1} = 12 \pm 2$ atm^{-1} and $K^I_{B1} = 50 \pm 9$ atm^{-1}. We conclude that ligand structural flexibility (for stabilization of a Cu(I)−CO center with nonplanar geometry) is a more effective influence on CO-adduct formation than the increased donor basicity in the more rigid Damox^{2-} complex. One might also note that the decrease in $E_1 - E_2$ under CO is in itself indicative of positive cooperativity (ca. 4 kJ mol^{-1}) between the two copper centers in [Cu(Dambn)], for CO binding. The structural and spectroscopic details germane to the cooperativity will be addressed elsewhere.

A few other features also emerge from the redox results. Replacing −OHO− by −OB(F_2)O− raises the $E_{1/2}$ values by a few hundred mV,[22,42] while the more flexible butylene linkages raises the $E_{1/2}$ vs the propylene ones.[43,44] Similarly, the chelates analogous to [Cu_2(Dampn)]$^{2+}$ and [Cu_2(Dambn)]$^{2+}$ but prepared from 2,6-diformyl-4-*tert*-butylphenol show elevations in DMF of 133 and 2 mV for the two waves,[29] while those from 2,6-diformyl-4-methylphenol show elevations of 90 and 130 mV for the two waves in dimethyl sulfoxide.[45] In connection with these results, axial interaction with solvent molecules renders the redox potentials quite solvent-sensitive, as is seen from the progression of the $Cu^{II}Cu^{II}/Cu^ICu^{II}$ $E_{1/2}$'s for [Cu_2(Dampn)]$^{2+}$ and [Cu_2(Dambn)]$^{2+}$ in DMF (−0.96, −0.80 V, respectively) vs CH_3CN (−0.74 and − 0.63 V, respectively[2]) and Cu_2(Damox)$_2$ in pyridine (−1.65 V) vs DMF (−1.22 V): the greater axial donicity stabilizes Cu(II) relative to Cu(I). Solvent dependence of $E_1 - E_2$ itself is apparent, others workers having commented on the consequences for the resulting comproportionation constant.[31] The full range of variation in this quantity (from 360 to 560 mV) across the complexes is expressed by just Cu_2(Damox)$_2$ between DMF and pyridine as solvents, while the effects of CO on the voltammograms are qualitatively quite solvent dependent as well.

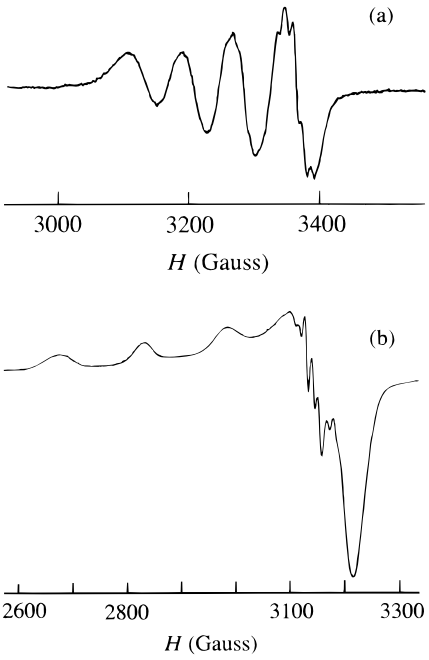

Figure 4. First-derivative EPR spectra of mixed-valence Cu^ICu^{II} complexes in MeCN: (a) [Cu_2(Dampn)]$^+$ at ambient temperature, with $g_o = 2.113$, $A_{o(Cu)} = 81 \times 10^{-4}$ cm^{-1}, and $A_{o(N)} = 14 \times 10^{-4}$ cm^{-1}. The shf-structure from the two imine N's on the Cu^{II} are most evident in the highest-field resonance line. (b) [Cu_2(Dambn)]$^+$ at 77 K. Overlapping Cu hf and imine-N shf contribute to the ∼8-line fine structure typical of a CuNN center, around 3150 G with a_N and $a_{\perp Cu} \approx$ 13 G.

Cathodic $n = 1$ electrolyses of the EPR-silent CH_3CN solutions of [Cu_2(Dampn)]$^{2+}$ and [Cu_2(Dambn)]$^{2+}$ (the latter with NBu_4PF_6) at the appropriate potentials yielded the mixed-valence species [Cu_2(Dampn)]$^+$ and [Cu_2(Dampbn)]$^+$. The $S = {}^1/_2$, $I = {}^3/_2$ EPR spectra (Figure 4) obtained for these, each including shf-lines from two unsaturated nitrogen donor atoms in the $g_\perp$ region, characterize both complexes as being valence-localized at both ambient temperature and 77 K. These resonances for [Cu_2(Dampn)]$^+$ ($g_{||} = 2.222$, $A_{||} = 207 \times 10^{-4}$ cm^{-1}, $g_\perp = 2.05$) and [Cu_2(Dambn)]$^+$ (77 K, $g_{||} = 2.239$, $A_{||} =$ 177, $g_\perp = 2.05$; 295 K, $g_o = 2.117$, $A_o = 63 \times 10^{-4}$ cm^{-1}) may be compared with those[43] for planar *cis*-CuN_2O_2 chelates such as [Cu(Apmpn)] ($g_{||} = 2.243$, $A_{||} = 186$, $g_\perp = 2.10$ in CH_3CN) which indicate that the nonreduced Cu^{2+} centers retain their tetragonal stereochemistry. It is interesting to note that replacement of the acyl methyl groups by protons in [Cu_2(Dambn)]$^+$ is a major contributory factor for transformation of the system from a valence-localized to a valence-delocalized one at ambient temperature in CH_3CN,[45] acting as a reminder of the dramatic sensitivity of the delocalization rate to substituents (and solvent).[29]

Magnetochemistry. Variable-temperature magnetic susceptometry was performed for [Cu_2(Damox)$_2$] (**1**), [Ni_2(Damox)$_2$(MeOH)$_2$]·MeOH (**2**), [Ni_2(Damox)$_2$(Py)$_2$]·Py (**3**), [Cu_2(Damfb)] (**4**), [Cu_2(Dabox)$_2$] (**5**), [Ni_2(Dabox)$_2$(H_2O)$_2$] (**6**), [Cu_2(Dampn)](NO_3)$_2$·4H_2O (**9**), and [Cu_2(Dambn)](NO_3)$_2$·2H_2O (**11**). The

(39) (a) Addison, A. W.; Rao, T. N.; Sinn, E. *Inorg. Chem.* **1984**, *23*, 1957. (b) McDevitt, M. R.; A. W. Addison, A. W. *Inorg. Chim. Acta* **1993**, *204*, 141. This product of the diffusion coefficient and the medium's viscosity, $D\eta$, corresponds to $RT/6\pi Nr$, where r is the effective Stokes-Einstein radius (Semenikhin, O. A. Personal communication, 1996), whence $i_{p,rev}$ (μA) = 0.0125 $AC^*_o\upsilon^{1/2}n^{3/2}r^{-1/2}\eta^{-1/2}$ (mM, cgsu, r in Å).
(40) Addison, A. W.; Dalal, N. S.; Hoyano, Y.; Huizinga, S.; Weiler, L. *Can. J. Chem.* **1977**, *55*, 4191.
(41) Gagné, R. R.; Allison, J. L.; Ingle, D. M. *Inorg. Chem.*, **1979**, *18*, 2767.
(42) Addison, A. W.; Watts, B.; Wicholas, M. *Inorg. Chem*. **1984**, *23*, 813.
(43) (a) Yokoi, H.; Addison, A. W. *Inorg. Chem.* **1977**, *16*, 1341. (b) Sakaguchi, U.; Addison, A. W. *J. Chem. Soc., Dalton Trans*. **1979**, 600.
(44) Nanda, K. K.; Addison, A. W.; Butcher, R. J.; McDevitt, M. R.; Rao, T. N.; Sinn, E. *Inorg. Chem.* **1997**, *36*, 134.
(45) Mandal, S. K.; Thompson, L. K.; Newlands, M. J.; Gabe, E. J. *Inorg. Chem.* **1989**, *28*, 3707.

Table 8. Magnetic Data for the Complexes

complex	$-2J$, cm^{-1}	g	zJ', cm^{-1}	D, cm^{-1}	$\rho^{a,b}$
$[Cu_2(Damox)_2]$ (**1**)	554	2.15			$<10^{-6}$
$[Ni_2(Damox)_2(MeOH)_2]\cdot$ MeOH (**2**)	3.2	2.08	-0.69	4.66	2×10^{-4}
$[Ni_2(Damox)_2(Py)_2]\cdot$Py (**3**)	19.5	2.16	-2.33	15.82	1×10^{-3}
$[Cu_2(Damfb)]$ (**4**)	778	2.2			1.4×10^{-2}
$[Cu_2(Dabox)_2]$ (**5**)	738	2.11			1.4×10^{-2}
$[Ni_2(Dabox)_2(H_2O)_2]$ (**6**)	-5.1	2.17	-9.4×10^{-5}	9.55	7×10^{-5}
$[Cu_2(Dampn)](NO_3)_2\cdot 4H_2O$ (**9**)	656	2.13			$<10^{-6}$
$[Cu_2(Dambn)](NO_3)_2\cdot 2H_2O$ (**11**)	594	2.13			8×10^{-3}

[a] Fraction of paramagnetic impurity. [b] EPR data for $S = {}^1/_2$ copper(II) impurity centers: $[Cu_2(Damox)_2]$ $g_{\|} = 2.317$, $A_{\|} = 162 \times 10^{-4}$ cm^{-1}, $g_{\perp} = 2.061$; $[Cu_2(Dabox)_2]$, $g_{\|} = 2.205$, $g_{\perp} = 2.060$; $[Cu_2(Dabfb)]\cdot H_2O$, $g_{\|} = 2.206$, $g_{\perp} = 2.060$; $[Cu_2(Dampn)](NO_3)_2\cdot 4H_2O$, $g_{\|} = 2.251$, $g_{\perp} = 2.072$; $[Cu_2(Dambn)](NO_3)_2\cdot 2H_2O$, $g_{\|} = 2.251$, $g_{\perp} = 2.075$. When appropriate, these values were used for $\bar{g}$.

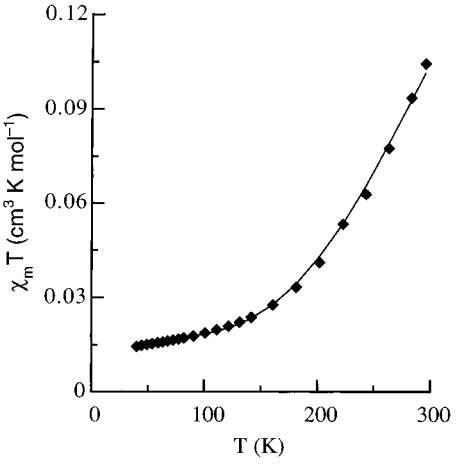

Figure 5. Variable-temperature magnetic data for $[Cu_2(Damfb)]$ (**4**). The points ◆ represent the experimental data, and the solid line represents the fit to eq 1.

results are summarized in Table 8, and some data are depicted as χT vs T plots in Figures 5−7.

For the dicopper(II) complexes $[Cu_2(Damox)_2]$ (**1**), $[Cu_2(Damfb)]$ (**4**), and $[Cu_2(Dabox)_2]$ (**5**) the $\chi_m T$ values increase with rising temperature, which indicates antiferromagnetic exchange interactions between the copper(II) centers. The variable-temperature magnetic susceptibility data for these complexes were fitted to the modified Bleaney−Bowers equation[46] (eq 2) using the isotropic exchange Hamiltonian ($H = -2JS_1\cdot S_2$) for the two interacting $S = {}^1/_2$ centers:

$$\chi_m(J,g,\rho) = \frac{2Ng^2\beta^2}{kT(3 + e^{-J/kT})}(1-\rho) + \frac{2Ng^2\beta^2\rho}{4kT} + 2tip \quad (1)$$

ρ and *tip* are the fraction of metal possibly present as a paramagnetic impurity and the temperature-independent paramagnetism per metal ion, respectively, the *tip* for Cu^{2+} being taken to be 6×10^{-5} cm^3 g $atom^{-1}$.[47] In all of the above copper(II) complexes, the metal ions are very strongly antiferromagnetically coupled, which is commonly observed in phenoxo-bridged dicopper(II) complexes of this type.[48,49] Figure 5 shows the temperature dependence of $\chi_m T$ for $[Cu_2(Damfb)]$ (**4**).

For dinuclear nickel(II) complexes, the zero-field splitting of the $S = 1$ ground state ($^3T_1$, $^3A_{2g}$, or $^3B_{1g}$) is often of the same order of magnitude as the electron spin-exchange integral (J).[50] Accordingly, a magnetic model (eq 2)

$$\chi_m(J,g,D,zJ',\rho) = \frac{2Ng^2\beta^2}{3k}\left[\frac{kF_1(J,D,T)}{kT - 4\,zJ'F_1(J,D,T)} + \frac{2kF'(J,D,T)}{1 - 4zJ'F'(J,D,T)}\right](1-\rho) + \frac{4\rho Ng^2\beta^2}{3kT} + 2tip \quad (2)$$

$$F'(J,D,T) = \frac{1}{D}F_2(J,D,T) + \frac{3C_2^{\,2}}{3J-\delta}F_3(J,D,T) + \frac{3C_1^{\,2}}{3J+\delta}F_4(J,D,T)$$

$$F_1(J,D,T) = \frac{1 + e^{4J/kT} + 4e^{4J/kT}e^{D/kT}}{2 + e^{D/kT} + e^{J/kT}e^{-\delta/kT} + e^{J/kT}e^{\delta/kT} + 2e^{4J/kT} + 2e^{4JkT}e^{D/kT}}$$

$$F_2(J,D,T) = \frac{2e^{4J/kT}e^{D/kT} + e^{D/kT} - 1 - 2e^{4J/kT}}{2 + e^{D/kT} + e^{J/kT}e^{-\delta/kT} + e^{J/kT}e^{\delta/kT} + 2e^{4J/kT} + 2e^{4JkT}e^{D/kT}}$$

$$F_3(J,D,T) = \frac{e^{4J/kT} - e^{J/kT}e^{\delta/kT}}{2 + e^{D/kT} + e^{J/kT}e^{-\delta/kT} + e^{J/kT}e^{\delta/kT} + 2e^{4J/kT} + 2e^{4JkT}e^{D/kT}}$$

$$F_4(J,D,T) = \frac{e^{4J/kT} - e^{J/kT}e^{-\delta/kT}}{2 + e^{D/kT} + e^{J/kT}e^{-\delta/kT} + e^{J/kT}e^{\delta/kT} + 2e^{4J/kT} + 2e^{4JkT}e^{D/kT}}$$

$$\delta = [(3J + D)^2 - 8JD]^{1/2}$$

$$C_1 = \frac{2.828D}{[(9J - D + 3\delta)^2 + 8D^2]^{1/2}}$$

$$C_2 = \frac{9J - D + 3\delta}{[(9J - D + 3\delta)^2 + 8D^2]^{1/2}}$$

is used which includes zero-field splitting (D), the usual intradimer exchange (J), and also an interdimer exchange parameter (zJ'). The resulting magnetic susceptibility equation, $\chi(g,J,D,zJ',\rho)$, derived by Ginsberg *et al.*[50] and corrected by Wen[51] has been used to fit the magnetic data for the dinickel-(II) complexes, **2**, **3**, and **6**. Equation 2 yields the susceptibility χ/mole of dinuclear complex, the term zJ' representing any

(46) Bleaney, B.; Bowers, K. D. *Proc. R. Soc. (London)* **1952**, *A214*, 451.
(47) Earnshaw, A. *Introduction to Magnetochemistry*; Academic Press: New York, 1968.
(48) Lambert, S. L.; Hendrickson, D. N. *Inorg. Chem.* **1979**, *18*, 2638.
(49) Mandal, S. K.; Thompson, L. K.; Nag, K.; Charland, J.-P.; Gabe, E. J. *Can. J. Chem.* **1987**, *65*, 2815.
(50) Ginsberg, A. P.; Martin, R. L.; Brookes, R. W.; Sherwood, R. C. *Inorg. Chem.* **1972**, *11*, 2884.

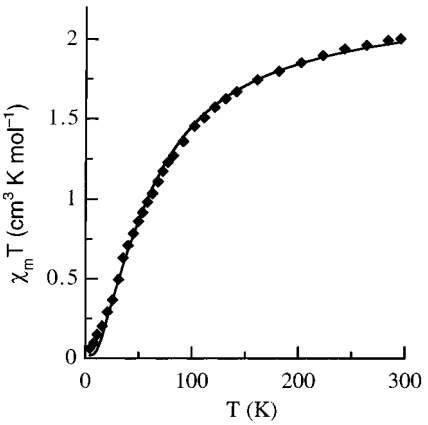

Figure 6. Variable-temperature magnetic data for $[Ni_2(Damox)_2(Py)_2]\cdot$Py (**3**). The points ◆ represent the experimental data, and the solid line represents the fit to eq 2.

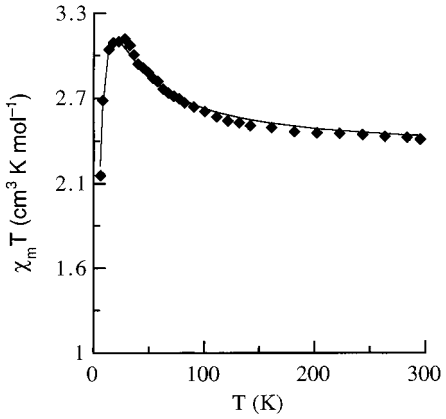

Figure 7. Variable-temperature magnetic data for $[Ni_2(Dabox)_2(H_2O)_2]$ (**6**). The points ◆ represent the experimental data, and the solid line represents the fit to eq 2.

interdimer interaction. The compositions and spectroscopic data evidence the nickel(II) geometry in $[Ni_2(Damox)_2(MeOH)_2]\cdot$MeOH (**2**), $[Ni_2(Damox)_2(Py)_2]\cdot$Py (**3**), and $[Ni_2(Dabox)_2(H_2O)_2]$ (**6**) to be square-pyramidal. The ground term for square-pyramidal nickel(II) is $^3B_{1g}$, for which no temperature-independent paramagnetism is expected,[47] so we have taken their *tip* values as zero. The *g*-values resulting from the least-squares fits are also in accord with expectation for nickel(II).[52] The complexes $[Ni_2(Damox)_2(MeOH)_2]\cdot$MeOH (**2**) and $[Ni_2(Damox)_2(Py)_2]\cdot$Py (**3**) exhibit antiferromagnetism, with $-2J$ values of 3.2 and 19.5 cm^{-1}, respectively. However, in $[Ni_2(Dabox)_2(H_2O)_2]$ (**6**) the two nickel(II) centers are coupled ferromagnetically ($-2J = -5.1$ cm^{-1}). The very evident decrease in μ_{eff} below 20 K (Figure 7) is due to population of the $M_s = 0$ state associated with the zero field splitting. In each case, the interdimer interaction term is, as expected, considerably smaller than the intramolecular coupling or the zero field splitting.

Nag and co-workers have proposed[53] a correlation between the Ni−$O_{phenoxo}$−Ni bridge angle and the extent of exchange coupling between nickel(II) centers in diphenoxo-bridged dinickel(II) complexes. According to their proposal, the angle for the crossover from antiferromagnetic to ferromagnetic exchange interaction is 97°. The crystal structure of $[Ni_2(Damox)_2(Py)_4]\cdot$2Py (**3a**), the precursor of $[Ni_2(Damox)_2(Py)_2]\cdot$Py (**3**), has a Ni−O−Ni angle of 96.9°. If the basic structure of **3a** is preserved in **3**, we should expect a weak ferromagnetic exchange interaction. Instead, we observe a moderate antiferromagnetic exchange interaction in **3** ($-2J = 19.5$ cm^{-1}) which suggests a Ni−O−Ni bridge angle of 99.6°. This kind of increase in bridge angle has been seen for phenoxo-bridged dinickel(II) macrocyclic complexes when the stereochemistry of the nickel(II) centers changes from octahedral to square-pyramidal.[53] The small values of $|2J|$ for **2** and **6** indicate that the Ni−O−Ni bridge angle in both the complexes is probably near 97°. Such an angle increase would be inevitable if one associates the axial ligands in the square-pyramidal complexes with a *trans*-relationship, as a result of the normal out-of-plane excursion of the metal ions.[54] This indeed appears to have been observed in the dicopper(II) systems.[55]

Acknowledgment. A.W.A. and K.K.N. thank Drexel University for support and Ms. S. Ghosh for assistance in growing crystals for diffractometry.

Supporting Information Available: Tables of crystal data, positional parameters, *U*-values, interatomic distances and angles, and least-squares planes for **3a** and **8** (22 pages). Ordering information is given on any current masthead page.

IC9712434

(51) Wen, T. Ph.D. Thesis, Memorial University of Newfoundland, Canada, 1988; p 53. *N*, *β*, *g*, and *k* have their usual meanings, so that when $N\beta^2/3k$ is taken as 0.125 erg K G^{-2} mol^{-1}, then, within the brackets, the values of *k*, F_i, and zJ' are self-consistently expressible in cm^{-1}-based units.

(52) Wertz, J. E.; Bolton, J. R. *Electron Spin Resonance: Elementary Theory and Practical Applications*; McGraw-Hill Book Co.: New York, 1972.

(53) Nanda, K. K.; Thompson, L. K.; Bridson, J. N.; Nag, K. *J. Chem. Soc., Chem. Commun.* **1994**, 1337.

(54) Hoskins, B. F.; Whillans, F. D. *Coord. Chem. Rev.* **1972**, *9*, 365.

(55) Mandal, S. K.; Thompson, L. K.; Newlands, M. J.; Gabe, E. J.; Nag, K. *Inorg. Chem.* **1990**, *29*, 1324.